Catalysis Science & Technology

COMMUNICATION

View Article Online
View Journal | View Issue

Cite this: *Catal. Sci. Technol.*, 2016, **6**, 6480

Received 19th May 2016,
Accepted 26th July 2016

DOI: 10.1039/c6cy01093h

www.rsc.org/catalysis

MOFs and their grafted analogues: regioselective epoxide ring-opening with Zr_6 nodes†

Nicholas E. Thornburg,[a] Yangyang Liu,[b] Peng Li,[b] Joseph T. Hupp,[b] Omar K. Farha[bc] and Justin M. Notestein*[a]

Zirconium(IV)-containing metal–organic framework (MOF) catalysts NU-1000 and MOF-808 were compared to analogous catalysts synthesized by grafting the nodes onto bare and functionalized silica. As-synthesized, calcined, and activated catalysts all exhibit similar selectivity in the ring-opening of 1,2-epoxyoctane with isopropanol, but MOF-808 gives exceptionally high rates and yields per gram catalyst.

Metal–organic frameworks (MOFs) have received recent attention as highly active catalysts with extraordinarily high porosity and nearly infinite synthetic tunability.[1–3] The organic linker units can be catalytically active[4,5] or can serve to attach or entrap molecular catalysts;[6] alternately, the inorganic nodes can be catalytic.[7,8] Defect sites have been recognized as critical to reactivity when the node is the catalyst.[9,10] For the Zr_6-benzoate[11] cluster-based MOFs such as NU-1000[12] (8-connected) and MOF-808[13] (6-connected), reactivity has been implicated in the relative Brønsted acidity of Zr–OH and Zr–OH_2 protons, a property related to both node connectivity and to the presence of open (labile) Zr cation coordination sites.[10] Defects must be generated and stabilized,[14,15] and this is often achieved *via* hydrothermal treatments following MOF synthesis.[16,17]

Here, we demonstrate that MOF nodes can be stabilized as active sites on other materials, and that there is a correspondence between the reactivities of MOF defect sites and supported clusters with other types of oxide defect sites, such as calcined supported oxides. Supported metal oxides are essential heterogeneous catalysts for many selective oxidation reactions key to commodity and fine chemical processes, and materials investigated here offer insight into building more well-defined defect sites in MOFs.

Separately, ring-opening of epoxides is a widely studied reaction in organic synthesis, catalyzed by both Brønsted[18] and Lewis acids.[19,20] Electron-poor terminal epoxides are challenging substrates to activate with Lewis acids, and studying trends in alkoxylation reactivity over heterogeneous Lewis acid catalysts provides insight into routes for upgrading conventional alkoxylation processes in industry.[19–23] In a few reports, homogeneous[24] and clay-supported[25,26] Zr^{IV} catalysts have given high regioselectivity to the more sterically challenging β-alkoxy alcohols. Separately, some of us have reported highly regioselective and enantioretentive epoxide activation using the Hf-NU-1000 MOF catalyst (isostructural to the Zr-based NU-1000) for CO_2 fixation, methanolysis and azidolysis[27] and for ring-opening with mild hydrides.[28] Opportunities exist for MOFs, supported metal oxides and other Lewis acids to facilitate these selective transformations, and here we investigate the ring-opening of 1,2-epoxyoctane with isopropanol as a model reaction over various ZrO_x-based materials.

The Zr_6-benzoate cluster node,[11] NU-1000[12] and MOF-808[13] were prepared according to literature protocol previously reported by some of us and by others. Structures were

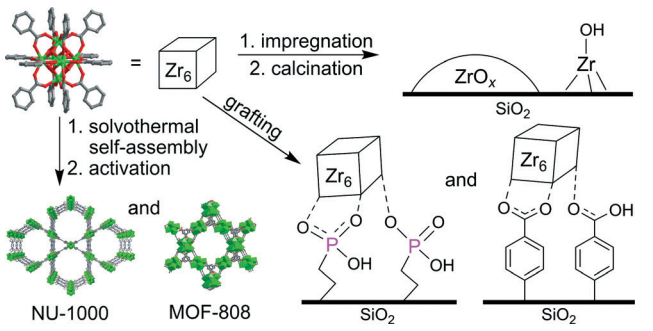

Scheme 1 General synthesis of Zr_6 cluster-based supported catalysts and MOFs.

[a] *Department of Chemical and Biological Engineering, Northwestern University, Technological Institute E136, 2145 Sheridan Road, Evanston, IL 60208, USA. E-mail: j-notestein@northwestern.edu; Fax: +1 847 491 3728; Tel: +1 847 491 5357*
[b] *Department of Chemistry, Northwestern University, Technological Institute K148, 2145 Sheridan Road, Evanston, IL 60208, USA*
[c] *Department of Chemistry, Faculty of Science, King Abdulaziz University, Jeddah, Saudi Arabia*

† Electronic supplementary information (ESI) available: Experimental procedures, instrumentation, PXRD, ^{31}P CP-MAS NMR, DRIFTS spectra, potentiometric titration curves, and ICP-OES data of spent catalysts. See DOI: 10.1039/c6cy01093h

confirmed using PXRD (Fig. S1–S3†). Zr_6 clusters were also immobilized onto SiO_2 surfaces functionalized with $-PO(OH)_2$ or –COOH moieties, generating catalysts "Zr_6–P-SiO_2" or "Zr_6–BA-SiO_2", respectively (Scheme 1). Ethylphosphonic acid-modified silica ("P-SiO_2," Sigma, 45–86 μm, 524 m^2 g^{-1}, 4.9 nm avg. pore dia., phosphonate loading of 0.94 mmol g^{-1} or 1.1 nm^{-2} by ICP-OES) is commercially available, whereas benzoic acid-functionalized silica ("BA-SiO_2") was synthesized *via* grafting of ethyl 4-(triethoxysilyl)benzoate to mesoporous silica gel (Selecto, 32–63 μm, 569 m^2 g^{-1}, 5.4 nm avg. pore dia., carboxylate loading of 0.42 mmol g^{-1} or 0.44 nm^{-2} from TGA) as reported by some of us elsewhere.[29,30] Functioning like a MOF linker, the supports' acidic functional groups serve as docking points for Zr_6 clusters, which graft at >80% yield from refluxing toluene, giving final loadings of 0.5–0.8 mmol Zr g^{-1}, equivalent to surface densities of ~0.6–0.8 Zr atoms nm^{-2} (Table 1).

Upon grafting, Zr_6 groups are irreversibly connected to the support. Diffuse reflectance UV-visible spectroscopy (DR UV-vis) gives evidence for the Zr_6 cluster in both Zr_6–P-SiO_2 and Zr_6–BA-SiO_2 based on growth of the feature at 275 nm, assigned to the ZrO_x LMCT band (Fig. 1). Similarly, NU-1000 and MOF-808 reveal comparable LMCT features between 270–280 nm. Optical edge energies of Zr_6–P-SiO_2, Zr_6–BA-SiO_2 and MOF-808 are all ~4.0 eV (Table 1), as determined by indirect Tauc plots,[31,32] suggesting the cluster maintains structural similarity across different support environments. The optical edge of NU-1000 is due to the 1,3,6,8-tetrakis(*p*-benzoic-acid)pyrene linkers, rather than the Zr_6 cluster. Independently, solid state ^{31}P CP-MAS NMR (Fig. S4†) indicates connectivity of the cluster to the P-SiO_2 support with the growth of a +22 ppm shift of a coordinated phosphorus,[33] while DRIFTS (Fig. S5†) indicates a shift in the P–O stretching frequency from 1010 cm^{-1} to 990 cm^{-1}, which is attributed to Zr–O–P connectivity.[34,35] Connections between phosphonates and these nodes are known to be strong.[36,37] Finally, potentiometric acid–base titration[38] shows the loss of a particular titratable acid site of the original P-SiO_2 support when the Zr_6 cluster is grafted (Fig. S6(a) and (e)†).

Next we studied the reactivity and selectivity of these materials in the ring-opening of 1,2-epoxyoctane with 4 eq. isopropanol at 55 °C and 1 mol% Zr (Scheme 2, Table 2). First,

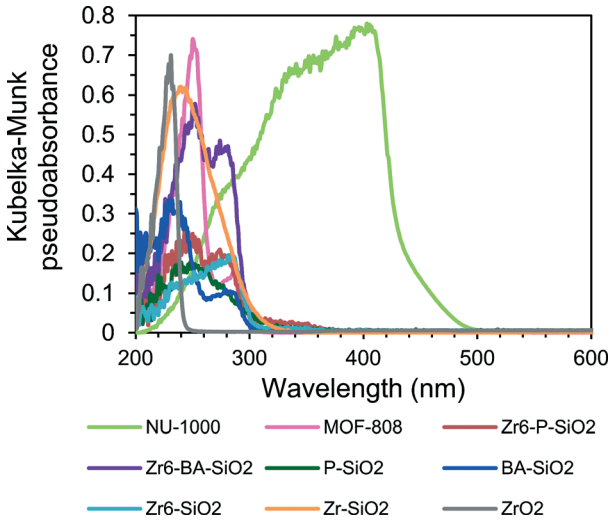

Fig. 1 Diffuse-reflectance UV-visible spectroscopy of ZrO_x-based catalysts.

NU-1000 and MOF-808 are catalytically inert without activation (Table 2, entries 2–3, respectively), the former with 0.5 M aq. HCl/DMF solution at 100 °C for 18 h and the latter with supercritical CO_2 drying followed by evacuation at 150 °C for 14 h.[12,13] Some of us have shown this step to be crucial in generating a preponderance of open (labile) Zr coordination site defects with greater exposed –OH and/or ligated $-OH_2$, responsible for strong acidity in the resulting catalysts.[10] Upon activation, both NU-1000 (Table 2, entry 4) and MOF-808 (Table 2, entry 5) gives a mixture of primary and secondary alcohols similar to that of general acid catalysis (Table 2, entry 1).

In contrast, grafted Zr_6 supported on modified SiO_2 is active as-synthesized. The same 'activation' with HCl actually reduces the catalytic activity, presumably by cleaving Zr_6 from the surface. Zr_6–P-SiO_2 (Table 2, entry 6) and Zr_6–BA-SiO_2 (Table 2, entry 7) give very similar selectivity to the MOF catalysts. Importantly, immobilization onto a support or within a framework plays a crucial role in the resulting reactivity, as the Zr_6 cluster itself is inactive as a homogeneous catalyst (Table 2, entry 10). Even though all are mildly acidic (Table S1†), no significant reaction occurs on the supports alone (Table 2, entries 11–12).

Table 1 Summary of catalysts

Catalyst	Zr precursor	Reference	BET S.A. (m^2 g^{-1})	Zr content[c]		Edge[d] (eV)
				mmol g^{-1}	nm^{-2}	
NU-1000	Zr_6[a]	12	2310	2.74	0.071	2.4
MOF-808	Zr_6[a]	13	1940	4.58	0.14	4.0
Zr_6–P-SiO_2	Zr_6[a]	This	524[b]	0.54	0.62	3.9, 3.1[e]
Zr_6–BA-SiO_2	Zr_6[a]	This	561[b]	0.78	0.84	4.0
Zr_6–SiO_2	Zr_6[a]	This	569[b]	0.22	0.23	3.9
Zr–SiO_2	dmCx-Zr	39	569[b]	0.21	0.22	3.7
ZrO_2	n/a	41	95.5	n/a	7.3	5.0

[a] Zr_6-benzoate cluster $Zr_6(OH)_4O_4(OOCPh)_{12}$·(PrOH)$(PhCOOH)_4$.[11] [b] BET surface area of support prior to Zr precursor deposition. [c] From ICP-OES of digested catalysts. [d] Determined from indirect Tauc plot.[31,32] [e] Shoulder feature.

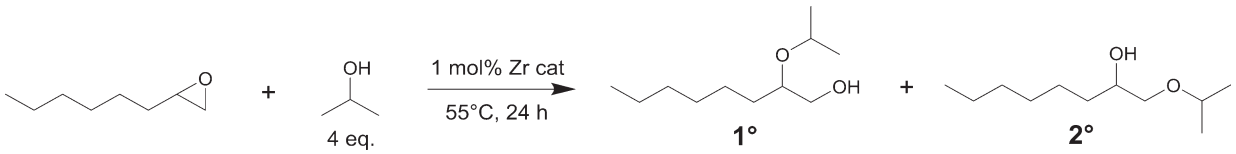

Scheme 2 Ring-opening of 1,2-epoxyoctane with 4 eq. isopropanol and 1 mol% Zr catalyst at 55 °C.‡

Table 2 Summary of 1,2-epoxyoctane ring-opening at 55 °C[‡,a]

Entry	Catalyst	Condition	Initial TOF[b] (min^{-1})	Initial rate[b] ($mmol\ g^{-1}\ min^{-1}$)	24 h yield (TON)	24 h yield ($mmol\ g^{-1}$)	Sel. to 2°/1°[c] (%)
1	HCl	37 wt% in H_2O	n/a	n/a	21	n/a	77/23
2	NU-1000	As-synthesized	0	0	0	0	—
3	MOF-808	As-synthesized	0	0	0	0	—
4	NU-1000	HCl-activated[d]	0.020	0.054	14	38	77/23
5	MOF-808	Dehydrated[d]	0.093	0.42	72	330	79/21
6	Zr_6–P-SiO_2	As-synthesized	0.057	0.031	24	13	80/20
7	Zr_6–BA-SiO_2	As-synthesized	0.022	0.017	9	7.0	81/19
8	Zr_6–SiO_2	Air-calcined, 550 °C	0.17	0.037	67	15	71/29
9	Zr–SiO_2	Air-calcined, 550 °C	0.18	0.041	82	17	73/27
10	Zr_6	As-synthesized	0	0	0	0	—
11	P-SiO_2	As-received (Sigma)	0	0	0	0	—
12	BA-SiO_2	As-synthesized	0	0	0	0	—
13	ZrO_2	As-received (Strem)	0	0	0	0	—

[a] Rates and yields from GC determination of total mmol (1° + 2°) per mmol Zr atoms or per g total catalyst. Note that TON, epoxide conversion and yield have the same numerical values under these conditions. [b] Product evolution over linear regime, generally first 30 min (see Fig. S7). [c] Zero selectivity to aldehyde rearrangement or hydrolysis products. Selectivity is independent of extent of reaction beyond 10% conversion (see Fig. S7). [d] See text for conditions.

Next we sought to compare these materials to a calcined, supported Zr oxide. For one material, the Zr_6 cluster was deposited onto bare SiO_2 *via* wetness impregnation in toluene ("Zr_6–SiO_2") at 0.22 mmol Zr g^{-1} (0.23 Zr atoms nm^{-2}). After solvent evaporation, the material was calcined in static air at 550 °C for 6 h. Separately, a dimethoxycalix[4]arene-Zr–Cl_2 ("dmCx-Zr") complex was grafted to SiO_2 at a nearly identical surface density, which upon calcination yields a material with highly dispersed, undercoordinated Zr oxide sites ("Zr–SiO_2"), recently reported by some of us for alkene epoxidation.[39] DR UV-vis of the calcined oxides display optical edges of 3.9 and 3.7 eV, respectively, similar to the grafted clusters and MOF-808, and in agreement with the absence of nanocrystallites of ZrO_2.[39–41] For ring-opening of 1,2-epoxyoctane, Zr_6–SiO_2 and Zr–SiO_2 (Table 2, entries 8–9, respectively) both give nearly identical initial rates and similar 24 h yields, at ~70% regioselectivity to the secondary alcohol product, marginally lower than the selectivity shown by the MOFs and their grafted analogues. Bulk ZrO_2 (Table 2, entry 13) is seen to be completely inactive.

All catalysts in this study have selectivity independent of conversion (Fig. S7†) and are stable to leaching and loss of crystallinity (for MOF catalysts) (Fig. S8, Table S2†). Differences in rate and conversion are therefore attributed to the availability of Zr atoms in each material to participate in catalysis. On a per-Zr atom basis, the initial rates (TOF) follow the trend of Zr–SiO_2 ~ Zr_6–SiO_2 > activated MOF-808 > Zr_6–P-SiO_2 > Zr_6–BA-SiO_2 ~ activated NU-1000. The calcined, pure oxide catalysts are expected to have a preponderance of highly dispersed, acidic Zr^{IV} sites, consistent with their high initial TOF and ultimate TON. The other catalysts are organic–inorganic hybrids and, by inference, have fewer defects that generate acid sites. Indeed, NU-1000 is known as a particularly stable MOF,[12,17] consistent with its low TOF. Alternate activation methods may increase its per-Zr reactivity.[41] Likewise, Zr_6–BA-SiO_2 is structurally similar to the defect-free and inactive Zr_6 cluster. MOF-808 is unique in that it has a moderate initial TOF, due to its inherently defective nodes,[13,42] but also a high final TON unlike, for example Zr_6–P-SiO_2, indicating that the MOF structure maintains active site accessibility even with extended reaction time.

The prior comparisons have been made on the basis of turnover numbers, per Zr atom. However, on mass basis, the MOF catalysts have much higher activity and final productivity than any of the grafted or calcined catalysts. In particular, MOF-808 has an extremely high loading of Zr_6 sites, giving it a 6-fold higher initial rate and a 20-fold higher final productivity than those of the reference Zr–SiO_2 or Zr_6–SiO_2 catalysts.

Conclusions

In summary, this study demonstrates the correspondences among acid catalysis carried out by the defects at ZrO_x nodes in MOFs, amorphous chemical analogues synthesized by grafting the ZrO_x nodes to appropriately decorated silica surfaces, and classical ZrO_x–SiO_2 supported oxides. In the MOFs and grafted materials, the incorporation of the Zr_6 node into

the solid material generates catalytically active defect sites from the otherwise inert Zr_6 node. One significant advantage of MOF catalysis is the very high density (mmol g^{-1}) of active sites that can be generated upon activation, resulting in excellent yields per g total catalyst. As a corollary, the high per-metal reactivity of conventional supported oxides should serve as an inspiration for building new generations of more selective and well-defined site architectures at high total loadings within MOFs.

The authors acknowledge financial support from the Dow Chemical Company. We thank Kurt Hirsekorn, Arjun Raghuraman and David Babb of the Dow Chemical Company for their useful conversations. ICP-OES analysis was performed at the Northwestern University Quantitative Bio-element Imaging Center. This work made use of the J. B. Cohen X-Ray Diffraction Facility supported by the MRSEC program of the National Science Foundation (DMR-1121262) at the Materials Research Center of Northwestern University. NMR experiments were performed at the IMSERC facility at Northwestern University with support from the NSF (DMR-0521267).

Notes and references

‡ Reaction protocol: 6.9 mmol 1,2-epoxyoctane was added to a 4 mL screw-top vial with a magnetic stirbar containing 0.069 mmol Zr catalyst, 28 mmol isopropanol and 7.0 mmol mesitylene (internal standard). The reaction vial was sealed, shaken at 700 rpm at 55 °C in a Glas-Col heated vortexer to initiate the reaction. Aliquots (50 μL) were withdrawn at specified time intervals using a syringe with a glass microfiber filter to remove suspended catalyst, diluted with 1.5 mL THF and analyzed using an Agilent HP 6890 GC-FID equipped with a Zebron ZB-624 capillary column (30 m × 0.25 mm × 1.4 μm) and quantified using calibrated standards. Mass balances >92%. See ESI.†

1 H. Furukawa, K. E. Cordova, M. O'Keeffe and O. M. Yaghi, *Science*, 2013, **341**, 1230444.
2 O. K. Farha and J. T. Hupp, *Acc. Chem. Res.*, 2010, **43**, 1166–1175.
3 J. Lee, O. K. Farha, J. Roberts, K. A. Scheidt, S. T. Nguyen and J. T. Hupp, *Chem. Soc. Rev.*, 2009, **38**, 1450–1459.
4 S. Kitagawa, S.-i. Noro and T. Nakamura, *Chem. Commun.*, 2006, 701–707, DOI: 10.1039/B511728C.
5 S.-H. Cho, B. Ma, S. T. Nguyen, J. T. Hupp and T. E. Albrecht-Schmitt, *Chem. Commun.*, 2006, 2563–2565, DOI: 10.1039/B600408C.
6 M. H. Alkordi, Y. Liu, R. W. Larsen, J. F. Eubank and M. Eddaoudi, *J. Am. Chem. Soc.*, 2008, **130**, 12639–12641.
7 K. Schlichte, T. Kratzke and S. Kaskel, *Microporous Mesoporous Mater.*, 2004, **73**, 81–88.
8 A. Henschel, K. Gedrich, R. Kraehnert and S. Kaskel, *Chem. Commun.*, 2008, 4192–4194, DOI: 10.1039/B718371B.
9 M. Vandichel, J. Hajek, F. Vermoortele, M. Waroquier, D. E. De Vos and V. Van Speybroeck, *CrystEngComm*, 2015, **17**, 395–406.
10 N. Planas, J. E. Mondloch, S. Tussupbayev, J. Borycz, L. Gagliardi, J. T. Hupp, O. K. Farha and C. J. Cramer, *J. Phys. Chem. Lett.*, 2014, **5**, 3716–3723.
11 G. Kickelbick, P. Wiede and U. Schubert, *Inorg. Chim. Acta*, 1999, **284**, 1–7.
12 J. E. Mondloch, W. Bury, D. Fairen-Jimenez, S. Kwon, E. J. DeMarco, M. H. Weston, A. A. Sarjeant, S. T. Nguyen, P. C. Stair, R. Q. Snurr, O. K. Farha and J. T. Hupp, *J. Am. Chem. Soc.*, 2013, **135**, 10294–10297.
13 H. Furukawa, F. Gándara, Y.-B. Zhang, J. Jiang, W. L. Queen, M. R. Hudson and O. M. Yaghi, *J. Am. Chem. Soc.*, 2014, **136**, 4369–4381.
14 G. C. Shearer, S. Chavan, S. Bordiga, S. Svelle, U. Olsbye and K. P. Lillerud, *Chem. Mater.*, 2016, **28**, 3749–3761.
15 Z. Fang, B. Bueken, D. E. De Vos and R. A. Fischer, *Angew. Chem., Int. Ed.*, 2015, **54**, 7234–7254.
16 F. Vermoortele, B. Bueken, G. Le Bars, B. Van de Voorde, M. Vandichel, K. Houthoofd, A. Vimont, M. Daturi, M. Waroquier, V. Van Speybroeck, C. Kirschhock and D. E. De Vos, *J. Am. Chem. Soc.*, 2013, **135**, 11465–11468.
17 A. J. Howarth, Y. Liu, P. Li, Z. Li, T. C. Wang, J. T. Hupp and O. K. Farha, *Nat. Rev. Mater.*, 2016, **1**, 15018.
18 R. E. Parker and N. S. Isaacs, *Chem. Rev.*, 1959, **59**, 737–799.
19 D. B. Williams and M. Lawton, *Org. Biomol. Chem.*, 2005, **3**, 3269–3272.
20 T. Ollevier and G. Lavie-Compin, *Tetrahedron Lett.*, 2004, **45**, 49–52.
21 J. Sebastian and D. Srinivas, *Appl. Catal., A*, 2014, **482**, 300–308.
22 R. J. Belner, *US Pat.*, 3278458, 1966.
23 R. J. Belner, *US Pat.*, 3427334, 1969.
24 M. Jafarpour, A. Rezaeifard and M. Aliabadi, *Helv. Chim. Acta*, 2010, **93**, 405–413.
25 Y. Permana, N. Ichikuni and S. Shimazu, *ITB J. Sci.*, 2012, **44**, 263–274.
26 Y. Permana, S. Shimazu, N. Ichikuni and T. Uematsu, *J. Mol. Catal. A: Chem.*, 2004, **221**, 141–144.
27 M. H. Beyzavi, R. C. Klet, S. Tussupbayev, J. Borycz, N. A. Vermeulen, C. J. Cramer, J. F. Stoddart, J. T. Hupp and O. K. Farha, *J. Am. Chem. Soc.*, 2014, **136**, 15861–15864.
28 C. J. Stephenson, M. Hassan Beyzavi, R. C. Klet, J. T. Hupp and O. K. Farha, *APL Mater.*, 2014, **2**, 123901.
29 P. A. A. Ignacio-de Leon, C. A. Contreras, N. E. Thornburg, A. B. Thompson and J. M. Notestein, *Appl. Catal., A*, 2016, **511**, 78–86.
30 N. J. Schoenfeldt and J. M. Notestein, *ACS Catal.*, 2011, **1**, 1691–1701.
31 D. G. Barton, M. Shtein, R. D. Wilson, S. L. Soled and E. Iglesia, *J. Phys. Chem. B*, 1999, **103**, 630–640.
32 J. Tauc and A. Menth, *J. Non-Cryst. Solids*, 1972, **8–10**, 569–585.
33 J. C. McKeen, Y. S. Yan and M. E. Davis, *Chem. Mater.*, 2008, **20**, 5122–5124.
34 A. Sinhamahapatra, N. Sutradhar, B. Roy, P. Pal, H. C. Bajaj and A. B. Panda, *Appl. Catal., B*, 2011, **103**, 378–387.
35 A. Raman, R. Quinones, L. Barriger, R. Eastman, A. Parsi and E. S. Gawalt, *Langmuir*, 2010, **26**, 1747–1754.
36 M. Taddei, F. Costantino, F. Marmottini, A. Comotti, P. Sozzani and R. Vivani, *Chem. Commun.*, 2014, **50**, 14831–14834.

37 P. Deria, W. Bury, I. Hod, C.-W. Kung, O. Karagiaridi, J. T. Hupp and O. K. Farha, *Inorg. Chem.*, 2015, **54**, 2185–2192.
38 R. C. Klet, Y. Liu, T. C. Wang, J. T. Hupp and O. K. Farha, *J. Mater. Chem. A*, 2016, **4**, 1479–1485.
39 N. E. Thornburg, A. B. Thompson and J. M. Notestein, *ACS Catal.*, 2015, **5**, 5077–5088.
40 J. D. Lewis, S. Van de Vyver, A. J. Crisci, W. R. Gunther, V. K. Michaelis, R. G. Griffin and Y. Román-Leshkov, *ChemSusChem*, 2014, **7**, 2255–2265.
41 S. Kouva, K. Honkala, L. Lefferts and J. Kanervo, *Catal. Sci. Technol.*, 2015, **5**, 3473–3490.
42 S.-Y. Moon, Y. Liu, J. T. Hupp and O. K. Farha, *Angew. Chem., Int. Ed.*, 2015, **54**, 6795–6799.